Available online at www.sciencedirect.com
SCIENCE DIRECT®
Journal of Nuclear Materials 337–339 (2005) 241–245
journal of nuclear materials
www.elsevier.com/locate/jnucmat

The effect of field reversal on the JET MkIIGB-SRP divertor performance in L-mode density limit discharges

A. Huber [a,*], J. Rapp [a], P. Andrew [b], P. Coad [b], G. Corrigan [b], K. Erents [b], W. Fundamenski [b], L.C. Ingesson [c], S. Jachmich [a], A. Korotkov [b], G.F. Matthews [b], Ph. Mertens [a], V. Philipps [a], R. Pitts [d], B. Schweer [a], G. Sergienko [a], M. Stamp [b], JET EFDA Contributors

[a] *Institut für Plasmaphysik, Forschungszentrum Jülich GmbH, EURATOM Association, Trilateral Euregio Cluster, 52425 Jülich, Germany*
[b] *EURATOM/UKAEA Fusion Association, Culham Science Centre, Abingdon Oxon OX14 3DB, UK*
[c] *FOM-Instituut voor Plasmafysica, Nieuwegein, The Netherlands*
[d] *CRPP, Association EURATOM-Confederation Suisse, EPFL, Lausanne, Switzerland*

Abstract

The effect of field reversal on the JET MkIIGB-SRP divertor performance has been investigated in L-mode density limit discharges. These experiments show that the direction of the magnetic field has a substantial effect on divertor physics, modifying the character of detachment and density limits. Reversal of the ion ∇B-drift direction away from the X-point results in a reduction of the density limit of about 15%. In contrast to forward field direction, the divertor parameters such as density and temperature as well as divertor radiation distribution and power at the divertor target become more symmetrical in the discharges with reversed field. The influence of different field configurations on the divertor performance has been analysed with respect to the dependence on density and heating power. The experimental observations of out–in asymmetry in target power as well as in the CIII-emission distribution is consistent with EDGE2D simulations, which include the effect of drifts.

PACS: 52.40.Hf; 52.25.Vy; 52.55.Fa
Keywords: Divertor asymmetry; Density limit; Divertor radiation; Detachment; Bolometer tomography

1. Introduction

Most of single-null divertor tokamak experiments show strong in–out asymmetries in particle and heat fluxes connected to asymmetries in divertor density, temperature and radiation. The analysis of these asymmetries is essential for the general understanding of divertor properties such as detachment, power exhaust, recombination, recycling and erosion/redeposition. As shown in many divertor tokamaks [1–5], the imbalances depend on the direction of the toroidal magnetic field (B_T) and are thus most probably a result of particle cross-field drifts. In this paper, we describe the effect of the toroidal field reversal on divertor plasma in

* Corresponding author. Tel.: +49 2461 612631; fax: +49 2461 612660.
E-mail address: a.huber@fz-juelich.de (A. Huber).

0022-3115/$ - see front matter © 2004 Elsevier B.V. All rights reserved.
doi:10.1016/j.jnucmat.2004.10.123

L-mode density limit discharges with different heating power input.

2. Experimental set-up

At JET, the spatial distribution of impurity radiation in the divertor has been analysed using three CCD cameras coupled to selectable interference filters (D_α-, CII-, CIII-emission lines). For this analysis, a 3D-tomographic reconstruction [6], reduced to a 2D-problem by the assumption of toroidal symmetry, has been performed. A survey spectrometer in the visible provides integrated D_α-, CII- and CIII-signals over both divertor legs and is used for cross-calibration and for comparison with the reconstructed 2D distributions of the line radiation.

In addition to the spectroscopic diagnostics, there is a poloidal array of fixed Langmuir probes (LP) in the inner and outer divertor targets that are used to measure local saturation current, electron density and temperature.

Power leaving the plasma is measured with a bolometer system for the radiated power and with an infrared camera for the power flux to plasma-facing surfaces. Additionally, the target power was measured using transient analysis of the thermocouples (TC) time traces. The bolometer system provides complete plasma coverage and was used for tomographic reconstruction of the distribution of total radiation.

3. Results and discussion

3.1. Experimental details and effects of the field reversal on density limit

The effect of the field direction on the divertor (MkIIGB-SRP) performance has been investigated on JET by B_T-reversal and plasma current direction simultaneously, so that the magnetic helicity remained constant. The measurements of n_e and T_e values at the top of the machine with Turbulent Transport Probe [7] (in the region of 6-50 mm outside the separatrix) show that these local plasma parameters had not been affected by the B_T-reversal. The global power balance was well satisfied for both field directions too, indicating the similarity of 'input power–plasma' coupling. For this study, L-mode density limit experiments have been performed with $B_T = 2.4$ T, $I_p = 1.7$ MA and with an additional NBI-power of 1.0–4.5 MW. The plasma density was raised steadily to the density limit by gas fuelling into the inner leg of the divertor at constant input power (P_{heat}). With continuous deuterium puffing, a high density, low temperature plasma forms inside the separatrix near the X-point (so-called X-point MARFE). The onset of an X-point MARFE, which is precursor to the ultimate density limit [8], appears at about 15% lower density for the pulse with reversed field direction ($B \times \nabla B\uparrow$). The lower density limit in the $B \times \nabla B\uparrow$ case could be explained by the fact that the plasma is stable if at least one of the divertor legs is attached. For both field configurations, the inner leg detaches (partially and totally) much earlier than the outer one and thus the outer divertor finally determines the density limit. The outer divertor in the reversed field discharge is colder than in forward field operation and correspondingly detaches earlier, what leads to lower density limit. Another possible explanation involves an increase of total radiation fraction ($\gamma = P_{rad}/P_{heat}$) (see Fig. 3(d)) in the case with reversed field configuration. An increase of the density limit with P_{heat} was observed for both field directions.

3.2. Field reversal effects on detachment

The direction of B_T has a substantial effect on the target density and temperature as well as on the detachment behaviour, as shown in Fig. 1. The field reversal leads to an increase of the n_e at the outer strike point (OSP), and at the inner strike point (ISP) as well. Contrasting to the behaviour of the $B \times \nabla B\uparrow$ discharge, the I_s^{ISP} current to the inner divertor in forward field operation remains at a constant level to begin with, but falls strongly above $\bar{n}_e \geqslant 2.5 \times 10^{19}\,m^{-3}$. This indicates that the inner divertor is partially detached (detachment takes place mostly at the separatrix) from the start. In

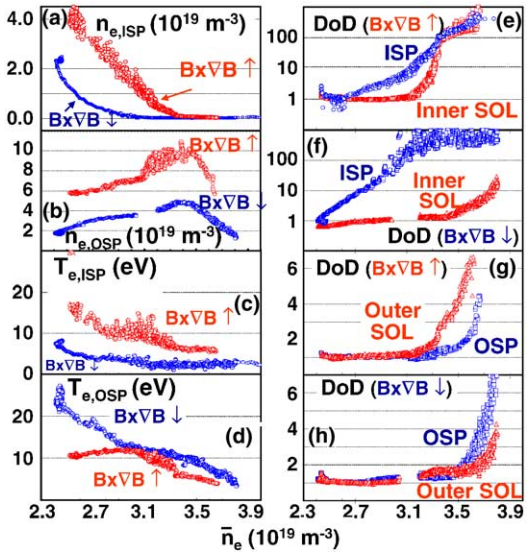

Fig. 1. Characteristics of the MkIIGB-SRP divertor plasma for both field directions as function of $\bar{n}_e$: (left column) electron density and temperature at ISP and OSP; (right column) the degree of detachment (DoD) of individual probes for both divertor legs.

the $B\times\nabla B\uparrow$ case, the I_s^{ISP} current increases at first in the same way as I_s^{OSP} current and after about $\bar{n}_e \geqslant 2.5\times10^{19}\,m^{-3}$ shows a continuously decreasing behaviour up to the discharge disruption. For high densities, $\bar{n}_e \geqslant 2.7\times10^{19}\,m^{-3}$, in reversed configuration we observe nearly balanced electron temperatures and for $\bar{n}_e \leqslant 2.7\times10^{19}\,m^{-3}$, the higher temperature side is inboard. Additionally, the degree of detachment (DoD) is included in this figure. The DoD is plotted for individual divertor LP and is defined as $DoD = C\times\bar{n}_e^2/I_s$ [9], where I_s is the ion saturation current of the corresponding probe. The behaviour of the DoD at ISP for forward case confirmed the earlier statement about a partially detached inner leg (at the separatrix) from the beginning. Partial and, correspondingly, total detachment for $B\times\nabla B\uparrow$ occur later in the inner divertor. Surprising is that, in contrast to the normal configuration ($B\times\nabla B\downarrow$), the outer scrape-off layer (SOL) in reversed field operation detaches first and then follows the detachment at the separatrix (see Fig. 1(g) and (h)). The ion saturation current I_s^{OSP} to the outer divertor, measured by LP at the strike point, initially increases for both field directions showing a factor of two larger values for pulse with ion ∇B-drift direction away from the X-point. Shortly before the reversed field discharge disrupts, the I_s^{OSP} drops dramatically: a MARFE forms inside the separatrix, which leads to a 'density limit' disruption. In the forward field operation, the I_s^{OSP} current begins to decrease slowly at a density of $\bar{n}_e = 3.3\times10^{19}\,m^{-3}$ which is much smaller than the density at onset of X-point MARFE ($\bar{n}_e = 3.8\times10^{19}\,m^{-3}$).

Fig. 2 shows the forward-reversed pairs of tomographic reconstruction of D_α-(top) and CIII-emission (middle) as well the total radiation in the divertor region at two different electron densities: $\bar{n}_e = 2.75\times10^{19}\,m^{-3}$ and $3.3\times10^{19}\,m^{-3}$. In the early phase of both pulses, the maximum of the hydrogen radiation is located near the target plates at the position of the strike zone. In forward field discharge we expect significantly more radiation from the inner leg than from the outer. On the other hand, the reversed field configuration shows a more symmetrical D_α-emission distribution in the divertor region. This is due to an increase of the ion flux into the outer divertor with a simultaneous decrease of T_e at target. With a reversal of the ion ∇B-drift direction, the CIII-emission in the outer leg decreases while increasing at the same time in the inner divertor. This is consistent with the behaviour of the T_e in the divertor: colder (warmer) outer (inner) leg leads to decrease (increase) of the physical sputtering of carbon. No significant changes are observed in the total radiation, between normal and reversed field direction plasmas. At $\bar{n}_e = 3.3\times10^{19}\,m^{-3}$ D_α detaches from the inner divertor for the $B\times\nabla B\uparrow$ configuration, in the forward field pulse both legs are still attached. Also the CIII-emission in the $B\times\nabla B\downarrow$ case remains in attached condition at the OSP.

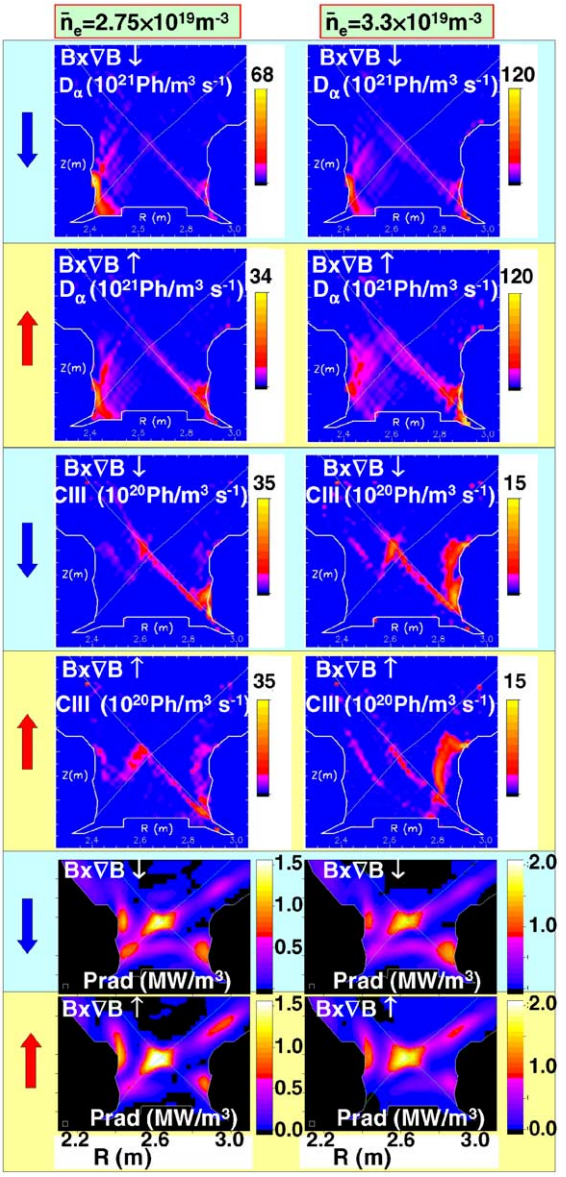

Fig. 2. Tomographic reconstruction of D_α- (upper rows) and CIII-emission (middle rows) as well the reconstruction of total radiated power (lower rows) in the divertor at two central averaged densities for both field directions.

3.3. Divertor asymmetries

Comparison of experimental data relating to in–out divertor asymmetry is illustrated in Fig. 3, which presents results of B_T-reversal on D_α-emission and CIII/D_α-ratio as well as radiated power and power to the target. The left column of the figure presents the dependence of divertor asymmetry on density and the right column on the power entering to the SOL (P_{SOL}). In contrast to reversed field operation, significantly higher

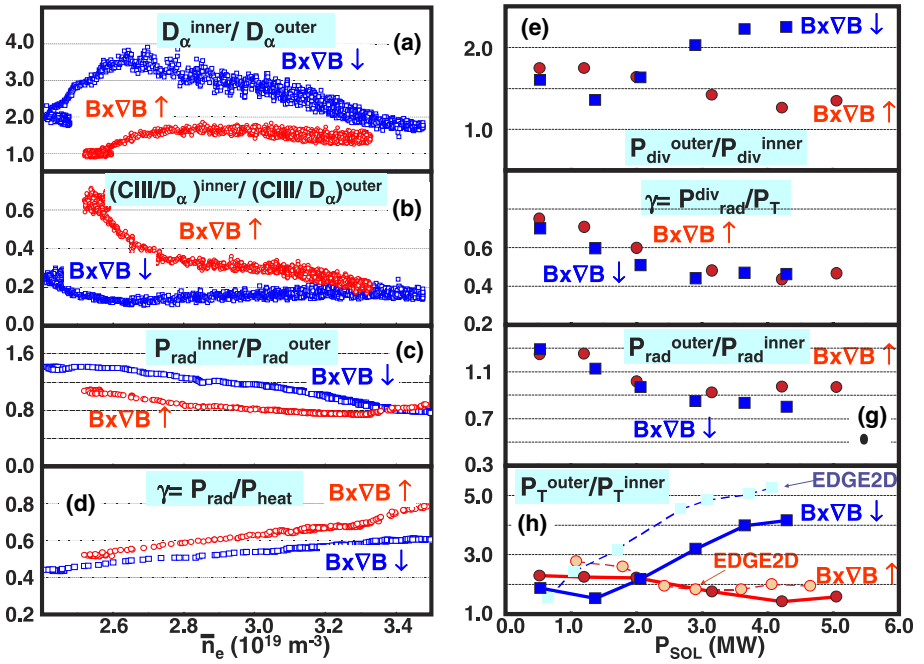

Fig. 3. Characteristics of divertor asymmetry versus $\bar{n}_e$ (left column) and P_{SOL} (right column) for forward and reversed field directions.

asymmetries were observed in the discharges with the ion ∇B-drift direction towards the X-point. With B_T-reversal, the asymmetries in D_α- and CIII-emissions are substantially reduced from $D_\alpha^{in}/D_\alpha^{out} = 3.5$ to $D_\alpha^{in}/D_\alpha^{out} = 1.4$ and from $(CIII/D_\alpha)^{in}/(CIII/D_\alpha)^{out} = 0.12$ to $(CIII/D_\alpha)^{in}/(CIII/D_\alpha)^{out} = 0.4$ for $\bar{n}_e = 2.7\times 10^{19}\,m^{-3}$, and $P_{NBI} = 1.8$ MW. The D_α-asymmetry in $B\times\nabla B\downarrow$ case is substantially suppressed at high densities and differs only slightly from the reversed field case. The CIII-asymmetry in reversed field discharge increases strongly with density and reaches the forward field value. In contrast to $B\times\nabla B\downarrow$, in reverse field regimes the asymmetries in D_α- and CIII-emissions do not depend significantly on the input power. Additionally, an increase of $\gamma = P_{rad}/P_{heat}$ is observed in the pulse with reversed field (Fig. 3(d)). The ratio of radiated power in the inner divertor to the power radiated in the outer divertor changes from 1.4 to 1.0 (more symmetrical in $B\times\nabla B\uparrow$ case) but at high densities no difference was observed. The right column of the Fig. 3 summarises the result from experiments with normal and reversed pulses, in which the heating power was increased in steps. Fig. 3(e) shows the ratio of the powers entering the outer and inner legs $P_{div}^{outer}/P_{div}^{inner}$, where P_{div} consists of the sum of power at the target (P_T), measured with thermocouples, and the power radiated in a corresponding divertor leg ($P_{rad,div}^{in/out}$). At low power the $P_{div}^{outer}/P_{div}^{inner}$ ratio is less sensitive to the B_T-reversal and varies between 1.5 and 2.0. However at high power the B_T-reversal effects strongly the $P_{div}^{outer}/P_{div}^{inner}$ ratio: the ratio increases for $B\times\nabla B\downarrow$ configuration up to value 2.3 while decreasing slightly to 1.25 with $B\times\nabla B\uparrow$. It follows that the out–in power asymmetry cannot be explained by an asymmetry in divertor radiation, which may otherwise be relevant for operation with lower P_{heat} or in high density regime, where the $P_{rad,div}^{in/out}$ is comparable with P_T. At higher input power though, divertor radiation cannot be significantly responsible for out–in power asymmetry. The target power asymmetries are probably a result of unequal power sharing between the targets, presumably due to classical drift effects [10]. In a recent review [11], the out–in power asymmetries were ascribed, in contradiction to our observation, to an asymmetry in divertor radiation (which was probably also caused by drifts). The out–in power asymmetry (P_T^{out}/P_T^{in}) at target is very sensitive to the B_T-direction, as shown in Fig. 3(h). Its increases with P_{SOL} from 2.0 to 4.1 for $B\times\nabla B\downarrow$ while decreases slightly from 2.25 to 1.5 in reversed field configuration.

The results of recycling (D_α) radiation for both field directions is largely consistent with results reported for H-mode plasma [12] indicating that classical drifts have relevance to different operating regimes.

3.4. Results of modelling

To understand the divertor asymmetry in forward and reversed field regimes, the EDGE2D/NIMBUS code [13], including all the classical particle drift terms was used. Poloidally and radially uniform transport coeffi-

cients were $D_\perp = 0.5\,m^2/s$ and $\chi_\perp = 1\,m^2/s$ for particle and energy respectively. Simulations with these coefficients produced good matches for both field directions with measured edge radial profile and temperature. Both physical [14] and chemical sputtering [15] control the intrinsic carbon content. As shown in Fig. 3(h), calculated asymmetry increases with P_{SOL} in $B\times\nabla B\downarrow$ case and decreases slightly in reversed field one, which matches well the experimental observation. The deviation between simulations and the experiment in the case of normal field operation could be explained by the fact that the code does not include heating of the divertor via radiation. Since the radiation, in first approximation, heats uniformly the inner and outer divertors, the P_T^{out}/P_T^{in}-ratio becomes smaller. No significant differences are observed in $P_{rad}^{out}/P_{rad}^{in}$-ratio, between $B\times\nabla B\downarrow$ and $B\times\nabla B\uparrow$ causes, confirming that target asymmetry presumably due to drifts and not due to different radiation behaviour. Analysis with EDGE2D/NIMBUS indicates that such power asymmetry may be result of drifts such as $\mathbf{E}\times\mathbf{B}$ and $\mathbf{B}\times\nabla\mathbf{T}$ (poloidal components) whose relative contribution scales as ρ_θ/λ_T, where ρ_θ is the ion poloidal gyro-radius and λ_T is the characteristic length for temperature. Besides the effects of drifts, the power asymmetry is influenced by effects that are independent of the $B\times\nabla B$-direction, such as geometry (larger outboard area, which alone leads $P_T^{out}/P_T^{in} = 1.7$ [10]), Shafranov shift and increased MHD-turbulence on the low field side (LFS). The use of poloidally varying radial transport coefficients ($D_\perp, \chi_\perp$) to simulate increased transport on the LFS leads to another increase of P_T^{out}/P_T^{in}-ratios (not shown in Fig. 3). The ion ∇B (and centrifugal) drifts were found to be insignificant in the simulation of L-mode discharges. The n_e- and T_e-asymmetries can be explained by the effect of a radial $\mathbf{E}\times\mathbf{B}$ drift [16] and of the poloidal drift in the private flux region (in $B\times\nabla B\downarrow$ case the particle flows from outer to inner divertor and this flow direction reverses in reversed field configuration).

Additionally, EDGE2D simulations successfully describe CIII-emission profiles, both for discharges with forward and reversed field directions.

4. Summary and conclusion

The analysis of plasma parameters in the divertor for both forward and reversed field discharges has led to the following conclusions:

- The density limit is approximately 15% lower in pulses with reversed B_T. An increase of the density limit with input power was observed for both field directions.
- The detachment behaviour in forward and reversed field pulses is very different. The inner divertor is detached from the start for normal field configuration. It detaches later in reversed field operations. In contrast to forward field operation, the outer SOL detaches first in discharges with ion ∇B-direction away from the X-point, and the OSP detaches later.
- The radiation of D_α and CIII becomes more symmetrical with B_T-reversal and varies slightly with electron density.
- The total radiation in the divertor shows similar pattern structures for both field directions. There is a slight increase of radiation at X-point in the case of reversed field configuration. The out–in divertor asymmetry of total radiation cannot be fully responsible for out–in heat power asymmetry.
- EDGE2D calculations with drifts successfully describe CIII-emission profiles as well as out–in target heat power asymmetry, both for discharges with forward and reversed field directions.

References

[1] F. Wagner, M. Keilhacker, The ASDEX and NI Teams, J. Nucl. Mater. 121 (1984) 103.
[2] D.N. Hill et al., J. Nucl. Mater. 176&177 (1990) 158.
[3] N. Asakura et al., J. Nucl. Mater. 220–222 (1995) 395.
[4] I.H. Hutchinson, et al, Plasma Phys. Control. Fus. 38 (1996) A301.
[5] A.V. Chankin et al., Plasma Phys. Control. Fus. 38 (1996) 1579.
[6] A. Huber et al., J. Nucl. Mater. 313–316 (2003) 925.
[7] C. Silva et al., Rev. Sci. Instrum. 75 (10) (2004) 4314.
[8] H.Y. Guo et al., Nucl. Fus. 40 (2000) 379.
[9] A. Loarte et al., Nucl. Fus. 38 (1998) 331.
[10] W. Fundamenski et. al., these Proceedings. doi:10.1016/j.jnucmat.2004.08.030.
[11] C.S. Pitcher, P.C. Stangeby, Plasma Phys. Control Fus. 39 (1997) 779.
[12] T.W. Petrie et al., J. Nucl. Mater. 313–316 (2003) 834.
[13] R. Simonini et al., Contrib. Plasma Phys. 34 (1994) 368.
[14] W. Eckstein, et al., Report IPP9/82, Max-Planck-Institut für Plasmaphysik, Garching, 1993.
[15] A.A. Haasz et al., J. Nucl. Mater. 248 (1997) 19.